Proceedings of the 35th European Safety and Reliability & the 33rd Society for Risk Analysis Europe Conference
Edited by Eirik Bjorheim Abrahamsen, Terje Aven, Frederic Bouder, Roger Flage, Marja Ylönen

doi: 10.3850/978-981-94-3281-3_ESREL-SRA-E2025-P8668-cd

Degradation Behavior and Failure Mechanisms of Silicone Rubber in a Simulated Marine Atmospheric Salt Spray Environment

Rui-Yuan Wang

School of Reliability and Systems Engineering, Beihang University, China.
E-mail: wangruiyuan2022@buaa.edu.cn

Wei-Fang Zhang

School of Reliability and Systems Engineering, Beihang University, China. E-mail: 08590@buaa.edu.cn

Silicone rubber, widely used as a sealing material in aerospace and marine equipment, plays a crucial role in ensuring operational reliability and safety. However, in the harsh marine atmospheric environment characterized by high salinity and humidity, the degradation behavior of silicone rubber differs significantly from that in inland environments, with the failure mechanisms still remaining unclear. To address the challenges of prolonged natural aging and unclear degradation behavior, this study established an accelerated aging platform in the laboratory and designed a neutral salt spray accelerated aging test. Through comprehensive analyses of macroscopic physical properties (weight loss, compression set, etc.), microstructure (XPS, SEM), and mechanical properties (tensile strength), the study systematically explores the performance degradation of silicone rubber under simulated marine atmospheric conditions with high salt spray and summarizes the failure mechanisms at various stages. The results indicate that the degradation of silicone rubber in a neutral salt spray environment can be divided into three stages, with Cl^{-} ions playing a pivotal role. In the initial stage, Cl^{-} rapidly penetrates the material; in the middle stage, the degradation slows down, and differentiation between the inner and outer layers becomes apparent; in the final stage, the degradation stabilizes, and the microstructure exhibits numerous through-holes, ultimately leading to material failure. These findings provide a basis for predicting the remaining service life of silicone rubber and help improve its reliability and durability in marine environments.

Keywords: Silicone rubber, accelerating test, degradation behaviour, failure mechanisms, marine atmospheric salt spray environment , reliability and durability.

1. Introduction

Environmental factors are the predominant external stressors responsible for the degradation and failure of equipment Chen et al. (2024); Ji et al. (2024). Research suggests that a significant proportion of material and structural failures in marine environments are influenced by climatic conditions, particularly high humidity, salt spray, and temperature fluctuations Jha (2013). While the failure mechanisms of electronic and control systems may differ, for elastomeric materials such as silicone rubber, prolonged exposure to these environmental stressors leads to degradation through oxidation, hydrolysis, and mechanical fatigue. The marine atmospheric environment is distinguished by its unique combination of high temperature, elevated humidity, intense ultraviolet radiation, and high salt spray concentration Asante et al. (2023); Olenin et al. (2024). Prolonged exposure to chloride ions, particularly sodium chloride, in high salt spray environments accelerates both chemical and physical material degradation, posing a serious threat to the structural integrity and functional reliability of equipment. Silicone rubber, a high-performance polymer, is extensively employed in critical sealing components of equipment, including aircraft and ships, due to its superior heat and ozone resistance. However, prolonged exposure to high salt spray environments inevitably degrades its performance over time, resulting in seal failure and jeopardizing the safe operation of equipment Wu et al. (2023); Wang et al. (2023). Therefore, a comprehensive investigation into the degradation behavior and failure mechanisms of silicone rubber in high salt spray environments is essential for accurate material lifespan prediction, design optimization, and enhanced equipment reliability.

Numerous studies have been conducted by domestic and international researchers on the degradation behavior and aging mechanisms of rubber under various environmental conditions. Kaneko et al. (2019) *et al.* revealed that, under high temperature, humidity, corona discharge, and ultraviolet (UV) radiation, the primary characteristics of silicone rubber degradation include the breakage of the cross-linked network and surface oxidation, which further exacerbate hydrophobicity loss and insulation performance decline. Tan et al. (2007) *et al.* focused on the compressive degradation behavior of rubber in the environment of proton exchange membrane fuel cells, uncovering the mechanism of surface microcrack formation and decomposition product generation under the synergistic effects of high temperature, humidity, and mechanical compression. Regarding the salt spray aging of rubber, Li et al. (2022) investigated the tribological behavior of nitrile rubber with varying acrylonitrile content reinforced with silica filler in a 3.5% sodium chloride solution by performing erosion and static swelling tests. The results indicated that the sodium chloride solution caused swelling of the nitrile rubber, increased hardness, and facilitated the penetration and diffusion of water and ions into the rubber, leading to altered material properties.

Despite significant progress in the study of the environmental adaptability and degradation of rubber materials, existing research still faces limitations, such as oversimplified environmental factors and a lack of systematic studies. To address these gaps, this study introduces key innovations, including the development of a laboratory-based accelerated aging test platform specifically designed for silicone rubber. Focusing on the typical marine salt spray environment of Hainan, China, accelerated aging experiments were conducted. By analyzing changes in macroscopic physical properties, microstructure, and mechanical performance, the degradation behavior and failure mechanisms of silicone rubber under high salt spray conditions were systematically examined. The findings provide a robust scientific foundation for optimizing material design and enhancing equipment reliability in such challenging environments.

The structure of this paper is organized as follows. Section 2 introduces the experimental materials and the design methodology of the accelerated aging tests. Section 3 presents and analyzes the experimental results. Section 4 elaborates on the aging mechanisms of silicone rubber. Finally, Section 5 summarizes the main conclusions of the study.

2. Materials and Accelerated Test Methods

2.1. *Materials*

The silicone rubber material was supplied by AVIC Beijing Institute of Aeronautical Materials, with its composition detailed in Table 1, where "Wt%" represents the weight percentage of each constituent. To investigate its degradation characteristics, various types of samples were prepared (as shown in Figure 1 (a)), and a custom-designed stainless steel compression device was used to measure the compression set at different aging intervals.

Table 1. Constituents of silicone rubber samples.

Constituents	**Wt%**
Fluorosilicone Rubber	62.5
Fumed silica	31.25
Structure Control Agent	4.375
Ferric Oxide	1.25
Curing Agent	0.625

2.2. *Design of Accelerated Salt Spray Aging Test*

To simulate the corrosive conditions of a tropical marine atmospheric environment, a neutral salt spray test was conducted to accelerate the aging of silicone rubber, as shown in Figure 2. The test was designed in accordance with the ISO 9227 standard, utilizing a 5% sodium chloride solution with a PH value maintained between 6.5 and 7.2. The

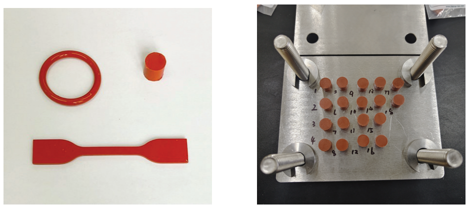

(a) Materials (b) Compression device

Fig. 1. Schematic diagram of silicone rubber samples and compression device used in accelerated aging tests.

test temperature was controlled at 35°C, with relative humidity maintained at no less than 85%, and the salt spray deposition rate kept at 0.0125–0.025 L/(h·m^2). Samples were positioned at an inclination of 20°–30° to prevent the accumulation of salt solution, which could interfere with the aging behavior. To examine the aging characteristics of silicone rubber over time, sampling intervals were set at 48, 96, 144, 288, 432, and 576 hours.

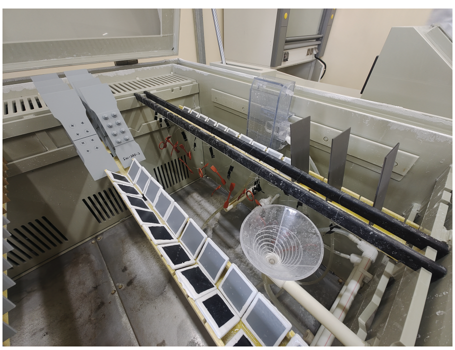

Fig. 2. Accelerated salt spray aging test equipment for silicone rubber.

2.3. *Degradation characterization*

2.3.1. *Macroscopic physical properties*

(1) Weight Loss

The weight loss (WL) of dumbbell-shaped and cylindrical silicone rubber samples was measured at specified aging intervals using a precision electronic balance (accuracy: 0.001 g). The WL percentage was calculated using the following Equation, where M_1 is the initial weight, and M_2 is the final weight. The results were averaged over three parallel samples after 24 hours under standard laboratory conditions.

$$\mathrm{WL} = \frac{M_1 - M_2}{M_1} \times 100\%. \tag{1}$$

(2) Compression Set

After specific aging intervals, samples were removed from the compression fixture and stabilized for 24 hours under standard conditions. The compression set (CS) was calculated using following Equation, where H_0 is the initial height, H_1 is the compressed height, and H_2 is the stabilized height after deformation Lou et al. (2022). Final results were averaged over three parallel samples.

$$\mathrm{CS} = \frac{H_0 - H_2}{H_0 - H_1} \times 100\%. \tag{2}$$

2.3.2. *Mechanical property test*

Mechanical degradation was assessed through uniaxial tensile testing at room temperature using a hydraulic MTS testing machine. Dumbbell-shaped specimens were tested with a gauge length of 25 mm and a tensile rate of 500 mm/min. Key mechanical properties, such as tensile strength, elongation at break, and elastic modulus, were determined. Post-fracture surfaces were analyzed with SEM to explore failure mechanisms.

2.3.3. *Microstructure analysis*

Microstructure analysis included ATR-FTIR, XPS, and SEM methods. ATR-FTIR was conducted using a Nicolet 6700 spectrometer (400 cm^{-1} to 4000 cm^{-1}, resolution 4.000 cm) with 32 scans and a diamond crystal ATR accessory for accuracy. XPS was used to assess Si, C, and O content with an Al K_α X-ray source (1486.6 eV, 14.8 kV, 1.6 A). SEM analysis was performed using an ELECT SUPER system (10 kV) to investigate fracture morphology and failure mechanisms, with samples sputter-coated with a platinum layer ($\sim$10nm) to enhance conductivity.

3. Results and Discussion

3.1. *Physical properties*

3.1.1. *Weight Loss*

Figure 3 illustrates the variation in weight loss rate over aging time under two different conditions. Specimens exposed to the salt spray environment

(Exposure to Salt Spray) exhibit a steady overall increase in weight loss rate, whereas specimens under compression in the salt spray environment (Under Compression in Salt Spray) show a distinct trend: rapid mass loss during the initial stage (48–144 hours), a decline during the middle stage (144–288 hours), and gradual stabilization in the later stage (after 288 hours).

This difference is primarily attributed to the interplay between mechanical stress and the release of degradation products. Mechanical stress under compression accelerates initial crack propagation but simultaneously restricts the release of volatile degradation products, resulting in a reduced mass loss rate during the middle stage. Furthermore, the compression device limits the surface area exposed to the salt spray, thereby slowing the degradation rate in the later stage.

Overall, whether exposed to the salt spray environment or under compression, the mass loss rate of silicone rubber exhibits minimal variation throughout the aging cycle (approximately 1%–1.5%). This highlights the excellent weather resistance of silicone rubber in salt spray conditions, demonstrating its exceptional chemical stability and resistance to salt spray-induced degradation.

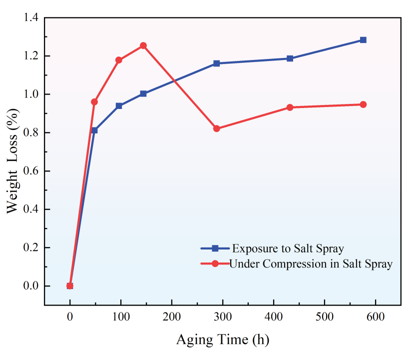

Fig. 3. Comparison of silicone rubber weight loss rate changes under different aging time and conditions.

3.1.2. *Compression Set*

Figure 4 illustrates the variation in the compression set (CS) of silicone rubber over aging time in a salt spray environment. During the initial stage (48–144 hours), the CS increased rapidly from 1.41% to 4.37%, indicating that chemical corrosion and mechanical stress in the salt spray environment significantly reduced the material's elasticity. In the middle and later stages (288–576 hours), the growth rate of CS slowed, eventually reaching 9.12%, suggesting that the degradation reactions gradually approached saturation.

Overall, the CS of silicone rubber increased continuously throughout the aging process in the salt spray environment. This result highlights the synergistic effects of chemical degradation and mechanical stress, which progressively diminished the material's elastic properties. It also indicates the limited ability of silicone rubber to maintain elasticity under prolonged exposure to salt spray conditions.

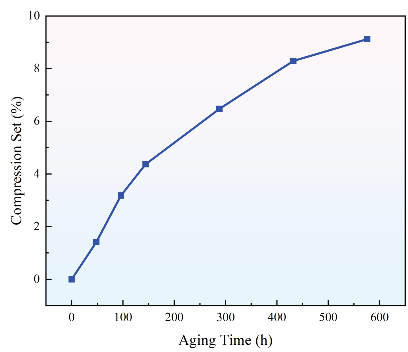

Fig. 4. Schematic diagram of the relationship between compression set and aging time of rubber samples.

3.2. *Mechanical properties*

Figures 5 illustrate the variation in tensile strength, elongation at break, and elastic modulus of silicone rubber during salt spray aging. The tensile strength (Figure 5(a)) decreased progressively over time, from 10.04 MPa in the unaged state to approximately 7.5 MPa after 576 hours, with the declining trend gradually stabilizing. The elongation at break (Figure 5(b)) decreased continuously, from 226.82% in the unaged state to approximately 140%. The elastic modulus (Figure 5(c)) exhibited an initial increase followed by a gradual decrease, rising from 5.04 MPa to approximately 5.3 MPa during the early stage

(0–144 hours) before declining to 4.4 MPa after 576 hours. These results demonstrate that the salt spray environment significantly influenced the mechanical properties of silicone rubber, leading to a reduction in tensile strength and elongation at break, as well as dynamic changes in elastic modulus.

The changes in mechanical properties are primarily attributed to the chemical degradation of silicone rubber caused by chloride ions and moisture in the salt spray environment. The reduction in tensile strength is attributed to oxidation and hydrolysis reactions on the material's surface, which break Si–O–Si bonds and reduce crosslink density, thereby weakening the material's load-bearing capacity. The decrease in elongation at break reflects the degradation of flexible molecular chains and the deterioration of the elastic network, resulting in diminished extensibility. The initial increase in elastic modulus is due to localized stiffening caused by surface degradation, while the subsequent decrease is associated with further internal structural degradation, leading to material softening. These changes align with trends observed in macroscopic properties, such as mass loss rate and compression set, underscoring the staged degradation effects of the salt spray environment on silicone rubber.

3.3. *Microstructure analysis*

3.3.1. *ATR-FTIR Analysis*

Figure 6 presents the infrared spectra of silicone rubber in the unaged state and after exposure to salt spray aging for different durations (48 hours, 288 hours, and 576 hours). In the unaged sample, characteristic absorption peaks of $-CH_3$ ($2968cm^{-1}$), Si–CH_3 ($1264cm^{-1}$), Si–O–Si ($1000cm^{-1}$), and Si–C ($798cm^{-1}$) are clearly visible, indicating the integrity of the silicone rubber's backbone structure and organic groups Wang et al. (2025). As aging progresses, the positions of these characteristic peaks remain largely unchanged; however, subtle changes in absorbance are observed. After initial aging (48 hours), the absorbance of the Si–O–Si peak slightly decreases, suggesting minor surface degradation. During intermediate aging (288 hours), the Si–CH_3 peak exhibits a weakening trend, accompanied by a reduction in the absorption intensity of Si–O–Si and Si–C. In the late aging stage (576 hours), the Si–O–Si and Si–C peaks weaken further, indicating damage to the backbone structure and deterioration of organic groups.

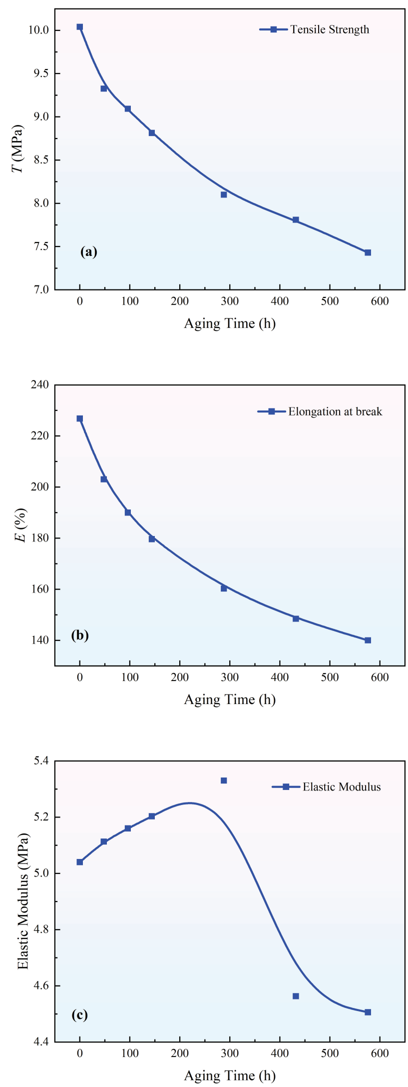

Fig. 5. Schematic diagram of the changes of different mechanical indices with aging time:(a) Tensile strength; (b) Elongation at break; (c) Elastic Modulus.

The observed changes in the infrared spectra reflect the chemical degradation of silicone rubber in a salt spray environment. During the initial aging stage, mild oxidation and hydrolysis reactions primarily occur on the surface, causing partial cleavage of Si–O–Si bonds. After 288 hours of intermediate aging, degradation extends deeper into the material, and the reduction in Si–CH_3 side groups indicates progressive oxidation and hydrolysis of the organic groups. In the late aging stage (576 hours), further decreases in the intensities of the Si–O–Si and Si–C backbone bonds reflect that degradation has penetrated deeper into the material, accompanied by the accumulation of oxidation products. Although no drastic changes are observed in the spectra, these localized chemical structural changes are sufficient to cause macroscopic performance degradation, including reduced mechanical properties and elastic recovery capabilities. The subtle spectral changes also suggest that silicone rubber exhibits a certain degree of resistance to salt spray degradation.

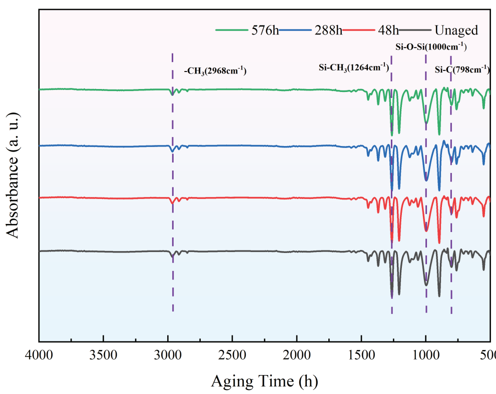

Fig. 6. Schematic diagram of infrared spectral bands of silicone rubber under different aging times.

3.3.2. *XPS Analysis*

Using XPS technology, the surface chemical composition changes of silicone rubber samples aged for 48 hours in a salt spray environment were analyzed (as shown in Figure 8(a)). Compared to the unaged sample, the main detected elements included C, O, Si, and trace amounts of Cl and Na. In the aged sample, the intensity of the C1s peak decreased significantly, while the intensities of the O1s and Si2p peaks increased, indicating a reduction in carbon content and an increase in oxygen and silicon contents on the surface. Quantitative analysis (as shown in Figure 7(b)) revealed that the carbon content declined markedly during the initial aging stage (0–96 hours) and then stabilized. Meanwhile, the oxygen content increased rapidly in the early stage and remained relatively stable during the later stages (144–576 hours). The silicon content showed a slight increase during the early stage of aging but exhibited a minor decline in the later stage.

These changes are primarily attributed to the cleaning and oxidation effects of the salt spray environment. During the early stage of aging (0–96 hours), the removal of surface carbon contamination layers and the oxidation of carbon chains by the salt spray resulted in a significant decrease in carbon content. Simultaneously, the formation of oxidation products, such as Si-OH and SiO_2, caused a rapid increase in oxygen content. Additionally, the cleaning effect of the salt spray exposed the Si-O-Si network, contributing to a slight increase in silicon content. In the later stage of aging (144–576 hours), the oxidation reaction approached saturation, leading to slower changes in oxygen content. Furthermore, salt deposition on the surface partially shielded the Si signal, resulting in a slight decline in silicon content. Overall, silicone rubber demonstrated good corrosion resistance in the salt spray environment, with relatively mild changes in surface chemical composition.

3.3.3. *SEM Analysis*

Figure 8 illustrates the fracture morphology of silicone rubber after tensile testing at different salt spray aging durations. The SEM images reveal that the fracture surface of unaged silicone rubber is smooth, displaying typical ductile fracture characteristics. With increasing aging time, the surface becomes progressively rougher, characterized by the appearance of more cracks and voids. After 48 hours of aging, localized microcracks and small voids are observed. By 288 hours, crack propagation becomes more extensive, the number of voids increases, and surface irregularities inten-

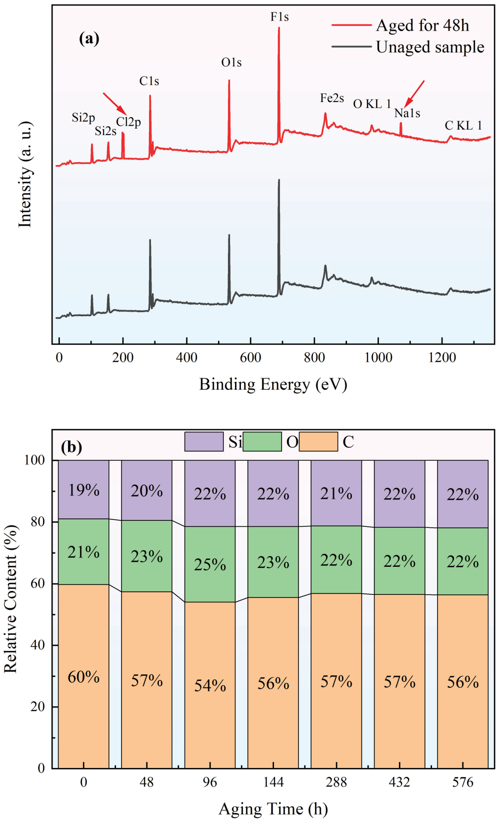

Fig. 7. Schematic diagram related to XPS analysis: (a) XPS survey spectrum of aging products in silicone rubber after 48 h of aging; (b) The relative content of C, O, and Si elements in silicone rubber at different aging times.

sify. At 576 hours, the fracture surface exhibits significantly more cracks and voids, indicating a transition toward brittle fracture characteristics.

The observed changes in fracture morphology are primarily attributed to chemical degradation caused by chloride ions and moisture in the salt spray environment. In the early stage (48 hours), degradation is predominantly confined to the surface, resulting in the formation of microcracks and voids. During the middle to later stages (288–576 hours), chloride ions penetrate deeper into the material, expanding the degradation zone, damaging the flexible structure, and reducing crosslink density. Consequently, the fracture behavior transitions toward brittle characteristics. These microscopic changes are consistent with the overall degradation trends observed in macroscopic properties.

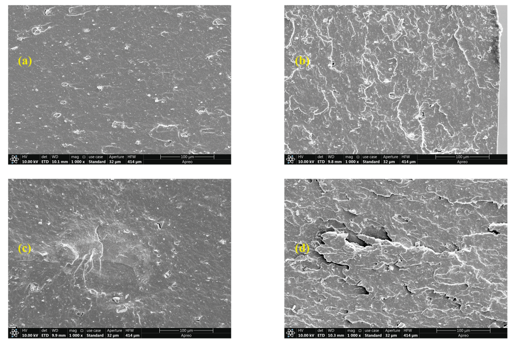

Fig. 8. Surface microscopic morphology of the silicone rubber after accelerate test for (a) unaged, (b) 48 h, (c) 288 h, and (d) 576 h.

4. Aging Mechanism Analysis

Based on the analysis of macroscopic physical properties, mechanical properties, and microstructural changes, the following aging mechanism is proposed:

The aging mechanism of silicone rubber in a salt spray environment is primarily driven by the synergistic effects of chemical degradation and physical processes. In the early stages of aging, chloride ions and moisture penetrate the surface, inducing the breakage of Si–O–Si bonds and oxidation of Si–CH_3 side groups. These processes are accompanied by the formation of localized oxidation products, leading to rapid surface performance deterioration. In the mid-to-late stages, degradation gradually extends into the material's interior, resulting in flexible chain breakage and reduced crosslink density, which significantly impact mechanical properties, such as tensile strength and elongation at break. Concurrently, the cleaning effect of the salt spray exposes more active regions, accelerating oxidation reactions, while salt deposition in the later stages partially inhibits further degradation. Microstructural characterization reveals a transition from ductile to brittle fracture, with increased cracks and voids on the fracture surface, reflecting the deepening of degradation.

Overall, the aging of silicone rubber in a salt spray environment follows a progressive deterioration from the surface to the interior, characterized by comprehensive changes in macroscopic performance, mechanical properties, and microstructure. This mechanism underscores the structural stability and degradation behavior of silicone rubber under salt spray conditions, providing a theoretical foundation for improving its weather resistance.

5. Conclusions

This study investigated the aging behavior and failure mechanisms of silicone rubber under simulated marine atmospheric salt spray conditions. The degradation process was divided into three stages: initial rapid penetration of Cl^- ions causing surface oxidation and hydrolysis, mid-stage differentiation between inner and outer layers with intensified microstructural damage, and final stabilization marked by through-holes and embrittlement.

Comprehensive analyses revealed that while weight loss remained minimal, compression set increased continuously, reflecting chemical degradation and stress effects. Mechanical properties declined significantly due to flexible chain breakage and reduced crosslinking density, with microstructural characterization confirming the pivotal role of Cl^- ions and oxidation products. These findings provide insights into silicone rubber's degradation mechanisms in marine environments and support strategies to enhance its durability and reliability.

Future research could focus on the following two aspects: (1) Silicone rubber operates in complex and dynamic environments, making it essential to explore degradation patterns under multi-factor coupling conditions; (2) Integrating laboratory accelerated test data with natural environment degradation data to validate the effectiveness of accelerated tests and provide more reliable assessments for practical applications.

Acknowledgement

The authors gratefully acknowledge that funding for this work was provided by Basic Technical Research Project of China under Grant JSZL2018601B004.

References

Asante, F., M. Bento, S. Broszeit, S. Bandeira, S. Chitará-Nhandimo, M. Amoné-Mabuto, and A. M. Correia (2023). Marine macroinvertebrate ecosystem services under changing conditions of seagrasses and mangroves. *Mar. Environ. Res. 189*, 106026.

Chen, Q., H. Wang, Y. Liu, Y. Shangguan, X. Ma, and Y. Cai (2024). Interpretable data-driven prediction methods for atmospheric chloride deposition rate. *Atmos. Environ. 334*, 120687.

Jha, W. C. U. (2013). *Weapons of War: Environmental Impact: Environmental Impact*. KW Publishers Pvt Ltd.

Ji, H., H. Wang, Q. Chen, X. Ma, and Y. Cai (2024). Corrosion behavior prediction for hull steels under dynamic marine environments by jointly utilizing lstm network and pso-rf model. *Ocean Eng. 300*, 117371.

Kaneko, T., S. Ito, T. Minakawa, N. Hirai, and Y. Ohki (2019). Degradation mechanisms of silicone rubber under different aging conditions. *Polym. Degrad. Stabil. 168*, 108936.

Li, D., Z. Leng, H. Wang, R. Chen, and F. Wellner (2022). Structural and mechanical evolution of the multiphase asphalt rubber during aging based on micromechanical back-calculation and experimental methods. *Materials & Design 215*, 110421.

Lou, W., C. Xie, and X. Guan (2022). Coupled effects of temperature and compressive strain on aging of silicone rubber foam. *Polym. Degrad. Stabil. 195*, 109810.

Olenin, S., M. Elliott, D. Minchin, and S. Katsanevakis (2024). Marine ecosystem health and biological pollution: Reconsidering the paradigm. *Mar. Pollut. Bull. 200*, 116054.

Tan, J., Y.-J. Chao, X. Li, and J. Van Zee (2007). Degradation of silicone rubber under compression in a simulated pem fuel cell environment. *J. Power Sources 172*(2), 782–789.

Wang, R.-Y., Z.-F. Dou, Z.-H. Liu, N. Li, X.-R. Liu, and W.-F. Zhang (2025). Research on ultraviolet degradation behavior and aging mechanisms of fluorosilicone rubber in simulated tropical marine atmospheric environment. *Polym. Degrad. Stabil.*, 111153.

Wang, R.-Y., C.-H. Wang, Y. Wang, and W.-F. Zhang (2023). Synergistic effects of multiple environmental factors on degradation of silicone rubber seals under marine atmosphere. *Materials 16*(21), 7013.

Wu, G., Y. Fan, Y. Guo, S. Xiao, Y. Liu, G. Gao, and X. Zhang (2023). Aging mechanisms and evaluation methods of silicone rubber insulator sheds: A review. *IEEE Trns. Dielectr. Electr. Insul.*.